Space Sci Rev (2015) 190:85–101
DOI 10.1007/s11214-014-0134-7

The Chang'e 3 Mission Overview

Chunlai Li[1] · Jianjun Liu[1] · Xin Ren[1] · Wei Zuo[1] · Xu Tan[1] · Weibin Wen[1] · Han Li[1] · Lingli Mu[1] · Yan Su[1] · Hongbo Zhang[1] · Jun Yan[1] · Ziyuan Ouyang[1]

Received: 29 August 2014 / Accepted: 30 December 2014 / Published online: 7 May 2015
© Springer Science+Business Media Dordrecht 2015

Abstract The Chang'e 3 (CE-3) mission was implemented as the first lander/rover mission of the Chinese Lunar Exploration Program (CLEP). After its successful launch at 01:30 local time on December 2, 2013, CE-3 was inserted into an eccentric polar lunar orbit on December 6, and landed to the east of a 430 m crater in northwestern Mare Imbrium (19.51°W, 44.12°N) at 21:11 on December 14, 2013. The Yutu rover separated from the lander at 04:35, December 15, and traversed for a total of 0.114 km. Acquisition of science data began during the descent of the lander and will continue for 12 months during the nominal mission. The CE-3 lander and rover each carry four science instruments. Instruments on the lander are: Landing Camera (LCAM), Terrain Camera (TCAM), Extreme Ultraviolet Camera (EUVC), and Moon-based Ultraviolet Telescope (MUVT). The four instruments on the rover are: Panoramic Camera (PCAM), VIS-NIR Imaging Spectrometer (VNIS), Active Particle induced X-ray Spectrometer (APXS), and Lunar Penetrating Radar (LPR). The science objectives of the CE-3 mission include: (1) investigation of the morphological features and geological structures of and near the landing area; (2) integrated in-situ analysis of mineral and chemical composition of and near the landing area; and (3) exploration of the terrestrial-lunar space environment and lunar-based astronomical observations. This paper describes the CE-3 objectives and measurements that address the science objectives outlined by the Comprehensive Demonstration Report of Phase II of CLEP. The CE-3 team has archived the initial science data, and we describe data accessibility by the science community.

Keywords Moon · Lunar · Spacecraft · Mission design

1 Introduction

The Chang'e 3 (CE-3) mission was successfully launched on December 2, 2013 at 01:30 local time as China's third lunar probe and the country's first lunar lander-rover mission.

✉ H. Li
lih@nao.cas.cn

1 National Astronomical Observatories, Chinese Academy of Sciences, 20A Datun Road, Chaoyang District, Beijing 100012, China

Previously two orbital probes Chang'e 1 (CE-1) and Chang'e 2 (CE-2) were launched in 2007 and 2010, respectively, as part of Phase I and first stage of Phase II of the Chinese Lunar Exploration Program (CLEP). The CE-3 mission was implemented as the second stage of Phase II of CLEP to explore the Moon from its surface. The successful landing of CE-3 at (19.51°W, 44.12°N) in Mare Imbrium on December 14, 2013 marked the first return of manmade spacecraft on the lunar surface since the former Soviet Union probe Luna 24 landed in Mare Crisium 37 years before (Kaydash et al. 2013).

The CE-3 rover has a planned mission phase of three months, and the lander's planned mission phase is one year. Science data from the CE-3 lander and rover will be deposited in the data archive center at the Ground Research and Application System (GRAS) of CLEP with open access to the exploration and science community.

To fulfill the science objectives of CE-3, the Chinese National Space Agency (CNSA) solicited proposals for CE-3 instruments and coordinated the processes of payload evaluation, construction and management. A total of eight science instruments were selected for the CE-3 mission. Science instruments on the lander include: Landing Camera (LCAM) (Liu et al. 2014b), Terrain Camera (TCAM) (Ren et al. 2014), Extreme Ultraviolet Camera (EUVC) (Chen et al. 2014), and Moon-based Ultraviolet Telescope (MUVT) (Wen et al. 2014). The four science instruments on the Yutu rover are: Panoramic Camera (PCAM) (Ren et al. 2014), VIS-NIR Imaging Spectrometer (VNIS) (He et al. 2014; Liu et al. 2014a), Active Particle induced X-ray Spectrometer (APXS) (Fu et al. 2014), and Lunar Penetrating Radar (LPR) (Fang et al. 2014) (Fig. 1).

In this review, we outline the science objectives and instrument capabilities of the CE-3 mission in Sect. 2 and summarize mission implementation in Sect. 3. In Sect. 4, we explain post-acquisition data processing; in Sect. 5, we provide information on how to access data from each instrument. Finally, a brief summarization of preliminary science results is included in Sect. 6.

2 CE-3 Science Mission Objectives

An initial formulation of CE-3 science objectives was conceived and outlined in the Comprehensive Demonstration Report of Phase II of CLEP submitted to the State Council in 2006. After the mission was approved in 2008, eight instruments were competitively selected, including Landing Camera (LCAM), Terrain Camera (TCAM), Extreme Ultraviolet Camera (EUVC), and Moon-based Ultraviolet Telescope (MUVT) on the lander, and Panoramic Camera (PCAM), VIS-NIR Imaging Spectrometer (VNIS), Active Particle induced X-ray Spectrometer (APXS), and Lunar Penetrating Radar (LPR) on the rover (Wu et al. 2014; Table 1). Due to the cancellation of several initially proposed instruments, the CE-3 science objectives were refined (Table 2) and the final formulation includes: (1) investigation of the morphological features and geological structures of and near the landing area; (2) integrated in-situ analysis of mineral and chemical composition of and near the landing area; (3) integrated exploration of lunar interior structure; and (4) exploration of the terrestrial-lunar space environment and lunar surface environment and lunar-based astronomical observations.

2.1 Morphological and Geological Investigation

Four instruments, LCAM and TCAM on the lander and PCAM and LPR on the rover, work in concert to investigate the morphological features and geological structures of and near the landing area.

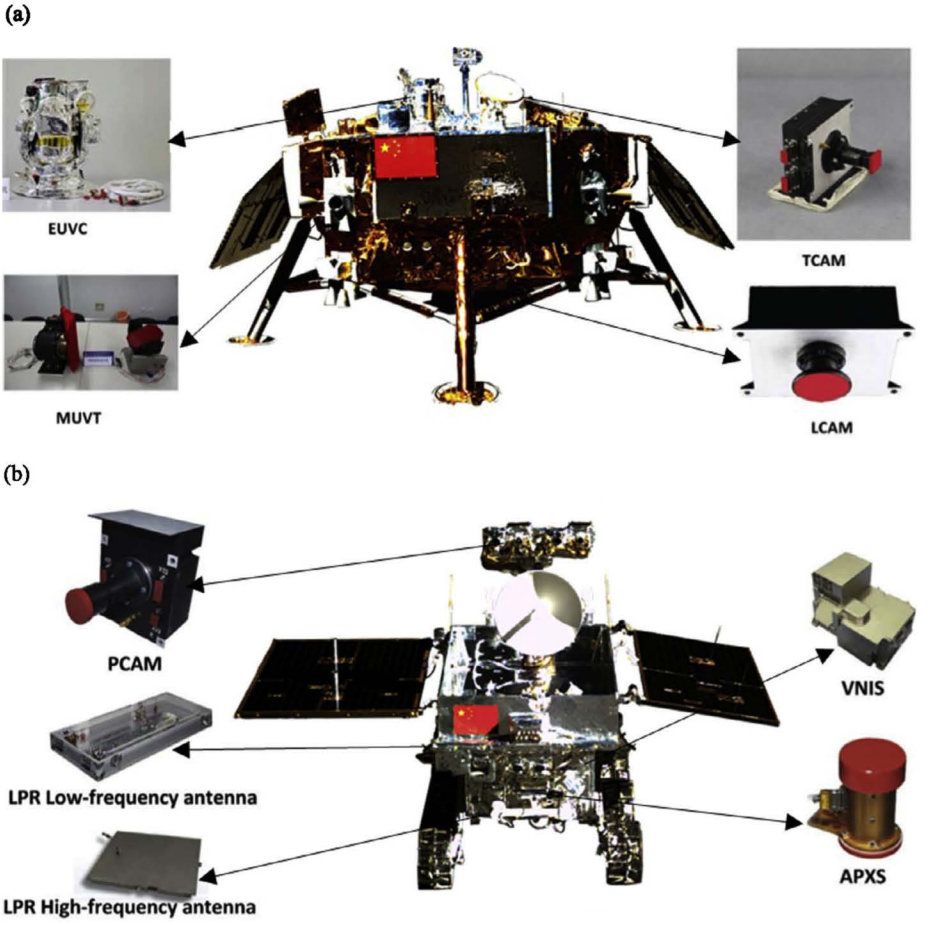

Fig. 1 Placement of science instruments on CE-3. (**a**) Extreme Ultraviolet Camera (EUVC), Moon-based Ultraviolet Telescope (MUVT), Landing Camera (LCAM), and Terrain Camera (TCAM) are mounted on the lander; (**b**) Panoramic Camera (PCAM), VIS-NIR Imaging Spectrometer (VNIS), Active Particle induced X-ray Spectrometer (APXS), and Lunar Penetrating Radar (LPR) are mounted on the rover

LCAM is capable of obtaining images with spatial resolutions between 3.2 mm and 1.62 m and with image widths between 1,656.9 m to 3.3 m at an elevation range of 2 km to 4 m during lander descent. In static imaging mode, TCAM can take 360° panoramic images of the landing area with a ±175° yaw angle. As it rotates on the horizontal plane, TCAM takes one image every 19°, or 19 images in one full circle; in two circles it captures 38 images for panoramic imaging. The imaging distance of TCAM is between 5 m and ∞. At a distance of 10–100 m, image resolution is 0.17–16.99 mm; at a distance of 600 m, average image resolution is 10 cm. Thus, TCAM can image the landing area within 600 m radius range for the purpose of morphologic and topographic analysis.

PCAM is able to obtain decimeter resolution continuous 3D image profiles approximately 2,000–2,200 m long and 1,400 m wide along the excursion path of the rover. LPR is designed to obtain radar data for information on decimeter-scale structures of the regolith

Table 1 Instrument performance parameters of CE-3's payload

Platform	Instrument	Major technical characteristics	Major performance characteristics
Rover	Panoramic Cameras (PCAM)	Spectral range: 420–700 nm Imaging modes: color and panchromatic Effective pixel number: 2,352 × 1,728 (color mode), 1,176 × 864 (panchromatic mode) FOV: 19.7° × 14.5°	Imaging distance: 3 m–∞
	Lunar Penetrating Radar (LPR)	Center frequency: 60 MHz (1st channel), 500 MHz (2nd channel) Band width: ≥40 MHz (1st channel), ≥450 MHz (2nd channel)	Depth range: ≥100 m (1st channel), ≥30 m (2nd channel) Vertical resolution: ~1 m (1st channel), ≤30 cm (2nd channel)
	VIS-NIR Imaging Spectrometer (VNIS)	Spectral range: 450–950 nm (Vis-NIR), 900–2,400 nm (IR) Spectral resolution: 2–10 nm (Vis-NIR), 3–12 nm (IR)	Detection distance: 0.7–1.3 m Quantization: 10 bit
	Active Particle induced X-ray Spectrometer (APXS)	Energy range: 0.5–20 keV Spectral resolution: 80–150 eV at 5.9 keV FWHM	Detection distance: 10–30 mm Accuracy for major elements: ≤15 %
Lander	Terrain Camera (TCAM)	Spectral range: 420–700 nm Imaging modes: color static, color video Effective pixel number: 2,352 × 1,728 FOV: 22.9° × 16.9°	Imaging distance: 5 m–∞ Quantization: 8 bit Video frame rate: 5–10 fps
	Landing Camera (LCAM)	Spectral range: 419–777 nm Effective pixel number: 1,024 × 1,024 FOV: 45° × 45°	Imaging distance: 4 m–∞ Quantization: 8 bit Frame rate: 10 fps
	Moon-based Ultraviolet Telescope (MUVT)	Spectral range: 245–340 nm Effective pixel number: 1,024 × 1,024 FOV: 1.36° × 1.36°	Detection limit: $\leq 1.13 \times 10^5$ counts/s/m^2 (30 s, 5σ) Resolution: 0.2 magnitude (within 5–13 magnitudes) Quantization: 8 bit
	Extreme Ultraviolet Camera (EUVC)	Center wavelength: 30.4 nm Band width: ≤5 nm FOV: 15°	Angular resolution: ≤0.1° Measurement range: 0.1–10 R

and meter-scale structures of the upper crust along the excursion path (planned length is approximately 800 m).

Science data obtained by LCAM, TCAM, PCAM, and LPR combined together are expected to help produce: (1) large-scale morphological and stereo-topographic maps of the landing area and excursion area; (2) large-scale regional geologic map with structure information; (3) 3D model of surrounding impact craters; (4) profiles showing structures of regolith and upper crust along the excursion path; and as a result, (5) improved understanding of regional morphology, tectonics, and formation and evolution of regolith and upper crust with the aid of additional compositional data.

Table 2 CE-3 science objectives with instrument measurement capabilities

Science Objective	Science Exploration Tasks	Contributing Instruments	
		Lander Instruments	Rover Instruments
Geomorphology and geological structure of and near the landing area	3D imagery Regolith thickness and subsurface structure	Landing Camera (LCAM), Terrain Camera (TCAM)	Panoramic Camera (PCAM), Lunar Penetrating Radar (LPR)
Mineralogy and chemical composition of and near the landing area	In-situ analysis of chemical composition (element content and distribution) In-situ analysis of mineralogical composition (mineralogical content and distribution) In-situ analysis of noble gases (isotopic content and distribution) Integrated analysis of mineral and energy resources		VIS-NIR Imaging Spectrometer (VNIS), Active Particle induced X-ray Spectrometer (APXS)
Terrestrial-lunar space environment and lunar-based, optical astronomical observation	EUV imaging of terrestrial plasmasphere Moon-based astronomical observation	Extreme Ultraviolet Camera (EUVC), Moon-based Ultraviolet Telescope (MUVT)	

2.2 Compositional Investigation

Two science instruments, APXS and VNIS on the rover, are selected to detect the mineralogical and chemical composition of and near the landing area.

Based on analysis of data obtained by APXS and VNIS, we hope to be able to obtain: (1) content and distribution of major elements in the excursion area; (2) content and distribution of major minerals in the excursion area; (3) regional "geochemical provinces" of regolith and upper crust with characteristic chemical and mineralogical composition, which can improve understanding of the chemical evolution of regional crust.

2.3 Space Environment and Astronomical Investigation

EUVC and MUVT onboard the lander are selected for the purposes of exploring the terrestrial-lunar space environment and lunar-based astronomical observation in near-ultraviolet (NUV), respectively.

EUVC can image the plasmasphere of the Earth from varied angles in the EUV wavelengths and obtain side view EUV images of the plasmasphere. During one lunar day, EUVC can collect data continuously for approximately 12 earth days, obtaining approximately 864×2 frames of continuous large FOV EUV images of terrestrial plasmasphere. It is expected to obtain for the first time a complete EUV record of changes in terrestrial plasmasphere throughout a geomagnetic storm cycle. This record provides first-hand data to study the dynamic processes during the initial phase, growth phase, and recovery phase of a geomagnetic storm, with potential to improve future space weather forecasting capability (Gonzalez et al. 1999; Mendillo 2006).

MUVT will make long-duration observations of selected areas of the sky in NUV, without atmosphere shielding and disturbance (Murphy and Vondrak 1993; Wang et al. 2011). Specifically, it can obtain continuous NUV images of objects at detection limits down to magnitude 13. Under ideal operational conditions, MUVT can obtain 60 × 24 × 11 images of selected areas of the sky during each lunar day in NUV wavelengths, as well as light curves of celestial bodies during the observation time period. The observable areas of the sky include the region 60°N pole-ward above the Moon, with a total area of ~2,762 square degrees, or approximately 6 % of the whole sky.

3 Science Mission Implement

CE-3 was launched on a Long March 3B rocket from the Xichang Satellite Launch Center in Sichuan Province at 01:30 (local time) on December 2, 2013, and was inserted into an initial near circular orbit (radius 100 km) after aerobraking on December 6. On December 10, CE-3 entered an elliptical orbit (15 km × 216 km). CE-3 stayed in this orbit for approximately four days before it landed at (19.51°W, 44.12°N) in northwestern Mare Imbrium at 21:11 (local time) on December 14 and sent back its first images taken by LCAM. The Yutu rover separated from the lander subsequently at 04:35 on December 15. During its first lunar-day observation, Yutu traversed from the lander-rover separation point along a semi-circle around the lander, allowing PCAM and TCAM to obtain color images of the lander and rover, respectively (Fig. 2). Yutu's subsequent traverse path is shown schematically in Fig. 3, with several important exploration points labeled for illustration. On the first lunar day, all science instruments on the rover and lander successfully obtained data as planned. On December 26, Yutu was powered off for the cold lunar night at exploration point N0108, approximately 18 m to the south of the lander.

Digital elevation models (DEMs) of the surrounding terrain were reconstructed based on image pairs obtained by PCAM at exploration points N0106, N0108 (same as N0201), N0203, and N0205 to guide traverse path planning (Fig. 3). On the second lunar day, at exploration point N0205, Yutu bypassed a boulder (measured at 1.5 m × 2.5 m), which previously had been selected as a geological exploration target, and changed traverse direction and headed northeastwards. Toward the end of the second lunar day on January 25th, Yutu encountered mechanical control issues, halting the rover's movement. The rover stopped at exploration point N0209, though all science instruments onboard both the rover and the lander continued to function well.

Members of the CE-3 Core Scientists Team, selected from a wide range of lunar experts from universities and the Chinese Academy of Sciences, help plan observations during the primary and extended mission and aid in the analysis of CE-3 science data, especially correlating results from multiple instruments to develop our understanding of the lunar surface and geological evolution.

4 Data Processing

Data obtained by the instruments onboard CE-3 are first packaged according to the Consultative Committee for Space Data Systems (CCSDS) standard before they are delivered from the lander and rover via time division multiplex access (TMDA) through multiple virtual channels (VC) to the two GRAS ground receiving stations located in Miyun and Kunming

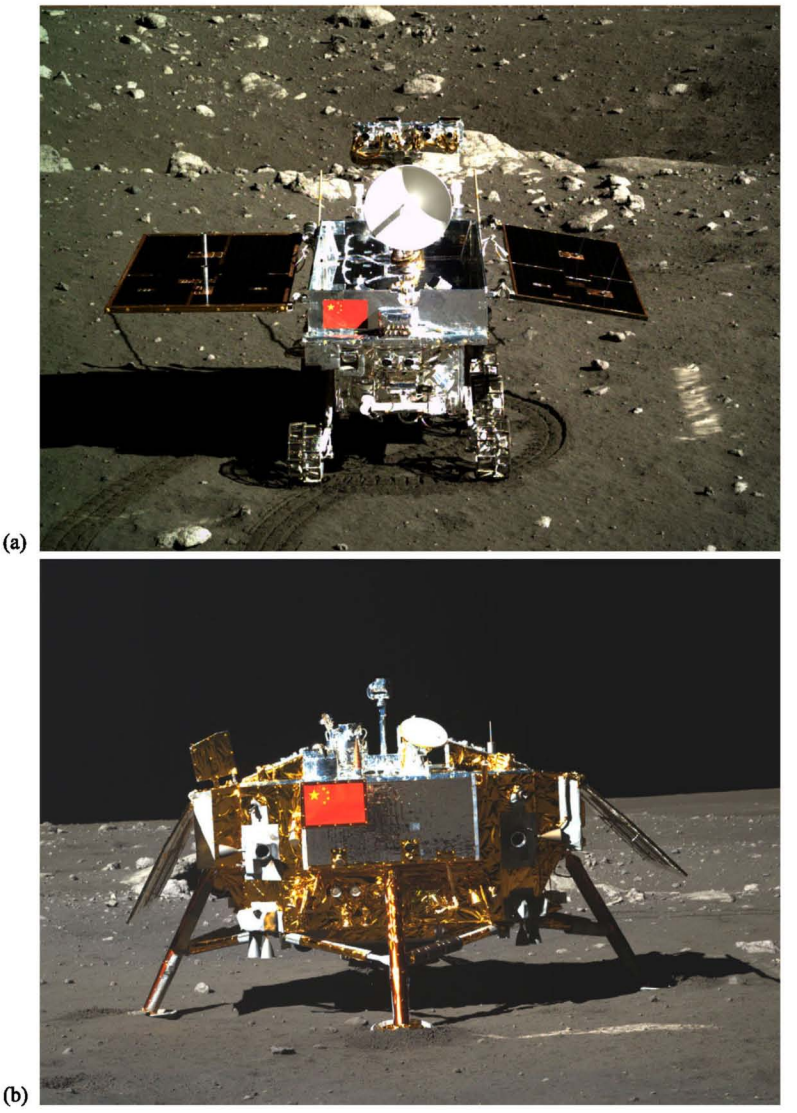

Fig. 2 The Yutu rover separated from the lander on December 15, approximately six hours after landing. **(a)** The Yutu rover as obtained by TCAM. Size of the Chinese flag is 192 mm × 128 mm; **(b)** Lander imaged by PCAM onboard the rover. Size of the flag on the lander is 480 mm × 320 mm

(Tan et al. 2014). Received data are then transmitted to GRAS Headquarters in Beijing for post-acquisition data processing. CE-3 data processing includes RS (Reed-Solomon) decoding and descrambling of the raw data, extracting science data of each instrument based on virtual channel identifier and instrument source package identifier, data optimization, format reforming, physical quantity conversion, and system correction and geometric information addition (Fig. 4). Science data products generated by the GRAS include Level 0 to Level 3 data (Table 3).

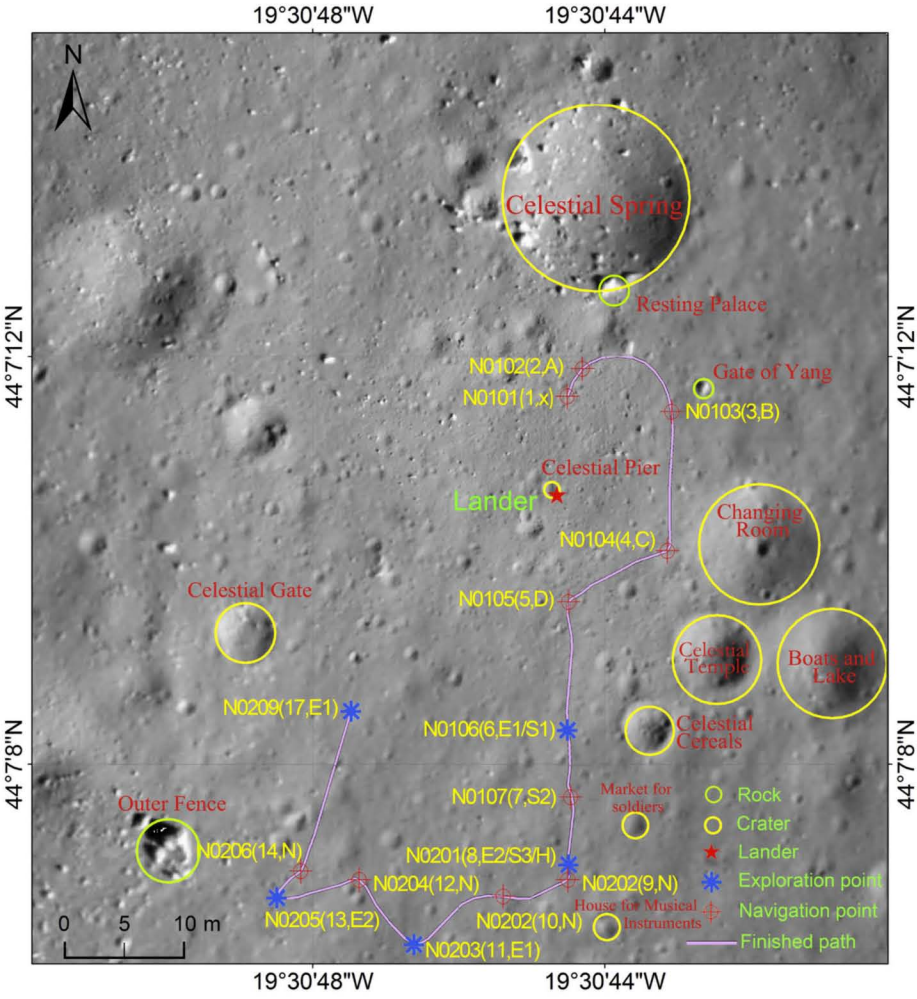

Fig. 3 Traverse path of the Yutu rover

4.1 Data Editing and Resampling (Level 0 and 1 Data Processing)

Level 0 and Level 1 data processing result in science data from each instrument divided by exploration periods. Specific procedures are as follows:

(1) Single station unpacking: at either ground receiving station, data are extracted from valid virtual channels based on downlink data format, and science data packets for each instrument are extracted based on individual instrument's application process identifier. In this step, data received by the two ground receiving stations are processed separately.
(2) Double station data compiling: for data from either station, valid data are extracted from science data packets and mosaicked into complete science data frames. Each data frame comprises exploration data and instruments parameters, as well as temporal information. Compressed data are also decompressed in this step. Then decisions are made about

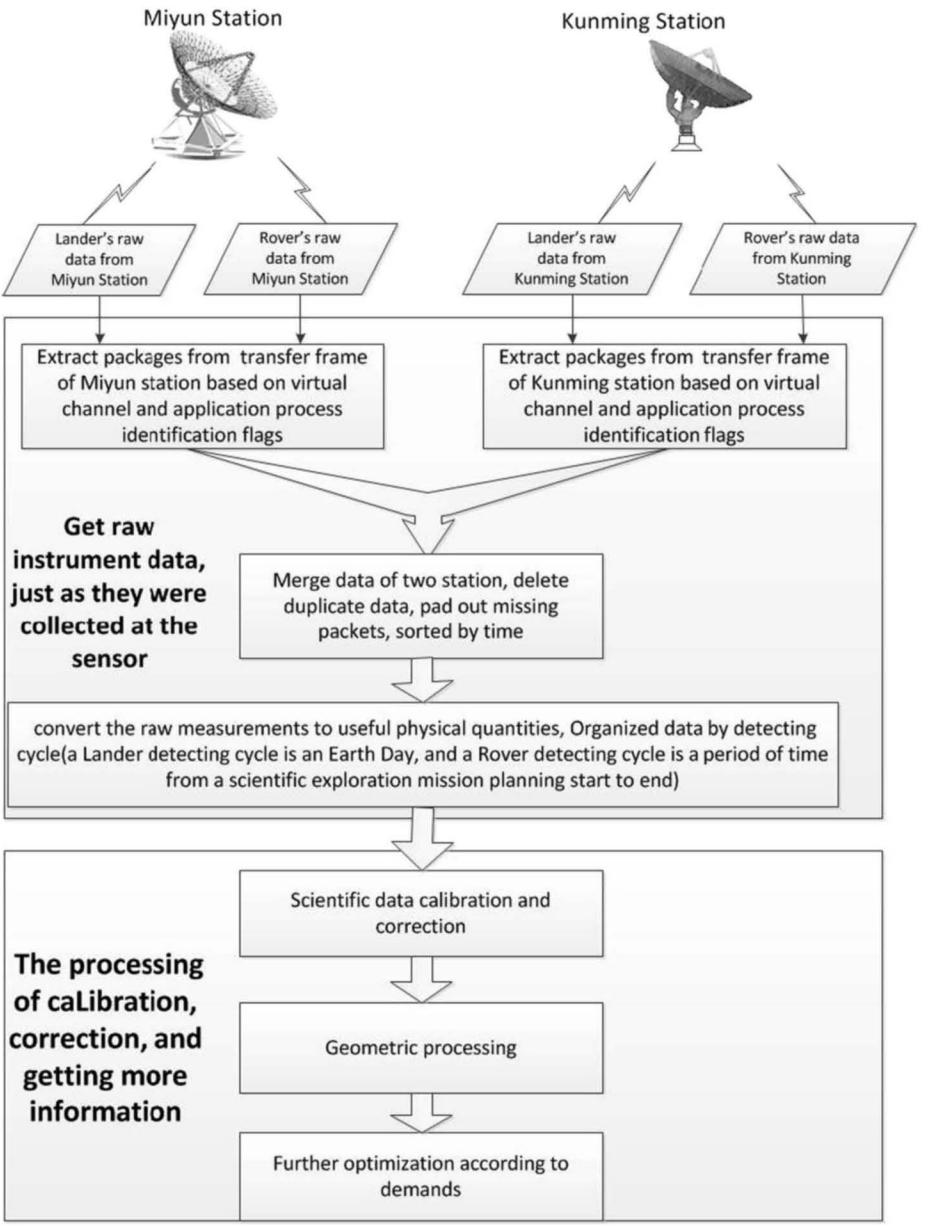

Fig. 4 CE-3 data processing pipeline

redundant data received by the two stations and only highest quality data are selected. Data are sequenced based on acquisition time and frame counts.

(3) Data integration: data from multiple transmission sequences are reorganized based on data acquisition time, such that each data file comprises all data collected in one exploration period. In particular, rover data downlinked from the lander are also integrated into one data file.

Table 3 CE-3 data processing levels

Data Level	Description	Comments
Raw data	Downlink data	Bit stream data
Frame data	Frame sequence after frame synchronization, descrambling, and RS decoding	
Level 0A	Payload data source pack	
Level 0B	Payload science data block	
Level 1	Data after physical quantity conversion, and mosaicked based on exploration periods	
Level 2	Data after payload system calibration and geometric calibration	Further divided into Level 2A, Level 2B, and Level 2C

4.2 Correction of Instrument Data (Level 2A Data Processing)

In Level 2A data processing, data of each instrument in different exploration periods (Level 1 data) are further corrected for scientific study. Level 2A processing for each instrument is explained below.

4.2.1 Level 2A Data Processing of LCAM

LCAM, mounted at the bottom of the lander, obtained image data during the lander descent from an elevation range of 12 km to 3 m. Level 2A data processing of LCAM mainly include: (1) extracting each individual frame image as one data file; (2) searching for corresponding calibration coefficient of each pixel based on image integration time (0.1 ms, 0.2 ms, 0.4 ms, 0.5 ms, 0.6 ms, 0.8 ms, 1.0 ms, 2.0 ms, 2.5 ms, 4 ms, 7.5 ms, 10 ms, 12.5 ms, and 15 ms), and multiply this coefficient with data DN values.

4.2.2 Level 2A Data Processing of TCAM

TCAM comprises a detector mounted on the lander camera pointing mechanism and an image compression board inside the payload electric control cabinet. Level 2A data processing of TCAM mainly includes: (1) extracting each individual frame image as one data file; (2) determining dark image based on image temperature and actual exposure time, and then subtracting dark image from scene image; (3) obtaining the relative calibration coefficient for each pixel for relative calibration; (4) normalization (TCAM works in different modes under varied lighting conditions, and the switching of modes causes prominent changes in image DN value; thus, image data taken under different TCAM modes must be normalized). Coefficients for R, G, and B channels are calculated so image exposure time is normalized to be 30 ms, without changing image data values.

4.2.3 Level 2A Data Processing of MUVT

MUVT images are $1{,}070 \times 1{,}027$, including two overscan areas: overscan1$[i, j]$ ($i \in [1, 6]$, $j \in [1, 1024]$) and overscan2$[i, j]$ ($i \in [1063, 1070]$, $j \in [1, 1024]$), and three dark current areas: dark1$[i, j]$ ($i \in [7, 22]$, $j \in [1, 1024]$), dark2$[i, j]$ ($i \in [1047, 1062]$, $j \in [1, 1024]$), and dark3$[i, j]$ ($i \in [1, 1070]$, $j \in [1025, 1027]$), and one valid pixel area: obj$[i, j]$ ($i \in$

[23, 1046], $j \in [1, 1024]$). Data processing only applies to those in the valid pixel area. Main processing procedures include: (1) overscan correction, (2) scattered light removal, and (3) flat-field correction.

4.2.4 Level 2A Data Processing of EUVC

EUVC, mounted on the top of the lander, will image the terrestrial plasmasphere using plasma resonance scattering at 30.4 nm. Level 2A processing of EUVC data includes: (1) radiance correction; (2) distortion correction; (3) image resampling (the 15° camera FOV and its optical angular resolution of 0.08° results in oversampling on the 1,500 × 1,500 detector; thus, pixels needs to be combined, and every 7 × 7 pixels are added together to obtain 214 × 214 images); (4) dark current correction; (5) image rotation (camera coordinates are shifted 60° from real world physical coordinates, and images need to be rotated counterclock wise 60°; pixel values after rotation are calculated through bilinear interpolation); (6) image cropping (images are cropped to a final size of 150 × 150 pixels).

4.2.5 Level 2A Data Processing of PCAM

PCAM comprises two identical cameras mounted on the rover mast. Level 2A data processing of PCAM includes: (1) dark current correction (obtain dark current coefficients based on information such as image gain and pixel location and subtract dark image); (2) radiance correction (divide image after dark current correction by radiance correction coefficient of each pixel); (3) work mode normalization (similar to TCAM, in this step, normalization coefficients are calculated so image exposure time is normalized to 10 ms, without actually causing changes to images).

4.2.6 Level 2A Data Processing of LPR

The low frequency antenna of LPR is a pole-shaped, dipole antenna placed at the end of the rover, while the high frequency antenna is a bow-tie antenna placed at the bottom of the rover. In Level 2A processing, DC component is removed from LPR data by applying a DC removal filter.

4.2.7 Level 2A Data Processing of VNIS

VNIS consists of two detectors: CMOS visible detector and SWIR near-infrared detector. Each data set requires different processing procedures.

Level 2A processing of CMOS data includes: (1) CMOS image salt-and-pepper noise removal; (2) dark current removal; (3) non-uniform correction; and (4) radiometric correction.

For SWIR, Level 2A processing procedures include: (1) removal of redundant short-wavelength IR data; (2) dark current removal; (3) SWIR detector temperature correction; and (4) radiometric correction.

4.2.8 Level 2A Data Processing of APXS

APXS is placed at the end of the rover mechanic arm. Level 2A processing of APXS data includes: (1) determining rover work mode (based on engineering data, it needs to be determined whether data are collected in calibration mode, rate meter detection mode, or in-situ detection mode); (2) calculating the distance between the detector and lunar surface; (3) converting energy number to energy; (4) dead time correction.

Table 4 CE-3 instrument geometric correction

Instrument	Geometric correction
PCAM/TCAM	Geometric information including observation vector of image four corner points and the center point, camera center position, camera rotation angle, solar incidence, solar azimuth, mast pitch angle and mast yawing angle
LPR	Position of reference point relative to the current position. Attitude of reference point relative to the current attitude
VNIS	Instrument parameters: focal length, pixel size, principal point position. Rover location and center point location. Geometric information including the incidence, azimuth and phase angles of the center point and four corner points
APXS	Geometric information including rover longitude and latitude, rover elevation, and rover attitude
LCAM	Geometric distortion correction using grid-point longitude and latitude spacing with 32 × 32 pixels, center point incidence angle, center point azimuth angle, center point phase angle, solar incidence angle, and solar azimuth angle
EUVC	Geometric information including camera observation vector in solar magnetospheric coordinate system
MUVT	Geometric information including gimbal azimuth, gimbal pitch, right ascension and declination in J2000

4.3 Geometric Correction (Level 2B Data Processing)

To correct geometric distortion caused by the cameras and provide lunar surface positioning information or geometric information, geometric correction needs to be performed through coordinate system transfers based on the position, attitude, and sensor parameters of the lander and rover, and lunar rotation and shape. Geometric information for CE-3 level 2B data processing is detailed in Table 4.

4.4 Need-Based Data Optimization (Level 2C Data Processing)

Currently, data obtained by three of the eight CE-3 science instruments, PCAM, TCAM, and LPR, have undergone Level 2C processing. Data from PCAM and TCAM are color-restored and color-corrected. Through color restoration, Red, Green, and Blue components for each pixel in the images are obtained. After color correction and white balance correction, Red, Green, and Blue components that reflect the true color of targets and meet human visual habits are obtained. For LPR Level 2C data processing, bandpass filtering is applied with a Finite Impulse Response (FIR) filter using the frequency sampling method.

5 Data Accessibility

To make the CE-3 observations accessible to both exploration planners as well as the science community, calibrated CE-3 data will be rapidly deposited into the Data Release System hosted by the Ground Research and Application System (GRAS) at http://moon.bao.ac.cn/ceweb/datasrv/dmsce2.jsp, where CE-1 and CE-2 data are also located.

CE-3 data are categorized into five levels including raw data and levels 0, 1, 2 and 3 data. Raw data (the demodulated and bit-synchronized, downlinked data stream) are organized by science payload into Level 0 data blocks after necessary processing, such as channel

Fig. 5 Panchromatic panorama at exploration point N106 (E) obtained by PCAM. A 16 m diameter crater lies to the north of the lander with boulders of relatively large size and high reflectance at the crater rim. To the west of the lander lies a 430 m diameter crater with a large number of boulders distributed on the crater wall and near the rim. In this panorama the Yutu Rover is 10 m away from the lander

processing, ordering, optimal splicing, deduplication, and source package header removal. Level 1 data generally consist of count rates converted into physical units, and Level 2 data are subsequently processed results after radiometric calibration, approximate geometric correction, photometric calibration, etc., which can be further divided into Levels 2A, 2B and 2C. Level 3 data products are appropriate for direct science application, such as imaging products with accurate geometric correction.

Typically, the first batch of high-level data, mainly Level 2 data, will be publically released after the expiration of the data proprietary period, which is usually six months after the beginning of the primary mission phase, and subsequent high-level data products will be delivered at regular intervals based on the progress of data production. Users can retrieve the specific files related to their research topic or download entire volumes containing chronologically organized data from the data release system. Low-level data, such as Levels 0 and 1, as well as raw data, are mainly used to verify instrument performance and algorithms by experts during the data proprietary period, after which such data can be obtained through written request according to the procedure described on the website mentioned above.

6 Preliminary Results

Of the eight science instruments onboard CE-3, LCAM was the first to be powered on. LCAM captured a total of 4,673 optical images of the surface from an altitude range of 2 km to 4 m at a rate of 10 frame/s. These images, with millimeter to decimeter resolutions, are employed to locate the landing site, reconstruct the lander descent trajectory, construct control points on the lunar surface, and assist in morphological analysis (Wang et al. 2014).

TCAM obtained panoramic images of the landing area by imaging the surrounding terrain as the camera rotated at three pitch angles. During each rotation, the camera obtained 20 frames either at horizontal position or at $\pm 30°$ pitch angles. A total of 120 frames of mm to decimeter resolution images of the landing area were obtained. Apart from imaging the lunar terrain, from an engineering point of view, TCAM also monitored the state of the rover as well as its traverse paths, and assisted in traverse planning and science target selection (Fig. 2). A panchromatic panorama was obtained at exploration point N106 (E) (Fig. 5).

PCAM obtained 360° stereo panoramas at the first three exploration points. Color panoramas were acquired at points N203 and N205 (Fig. 6). Three stereo image pairs were obtained at exploration point N209. These millimeter- to decimeter-resolution images are used to assist in the analysis of local morphological and structural characteristics (Li et al. 2014).

VNIS was powered on at four exploration points and obtained visible images and NIR spectral data of the regolith at points E, N203, and N205 (after calibration), with a total data volume of 350 MB. These spectra will assist in the analytical study of minerals in the

Fig. 6 Color panorama obtained by PCAM at exploration point N205. In the background is the lander located to the northeast of the rover, with rover tracks between them visible on the ground. In the foreground are the two antennas of Lunar ground-Penetrating Radar (LPR) installed on the rover

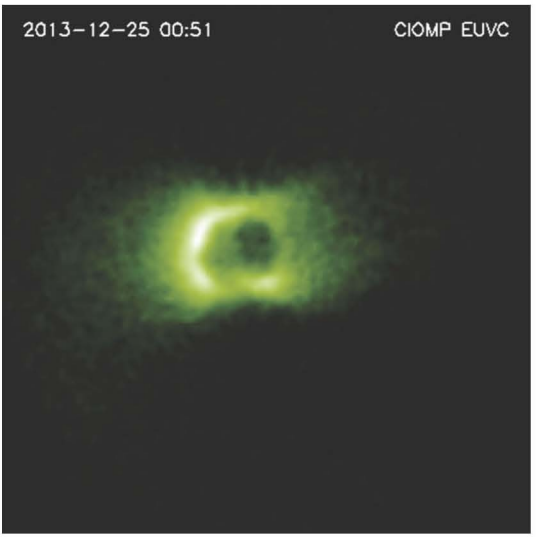

Fig. 7 Observation of Earth's plasmasphere by EUVC on December 25, 2013 after background removal. The plasmasphere, plasmapause, airglow and Earth's shadow can be seen in this image

lunar regolith. Energy spectra acquired by APXS at points N202 and N205 will assist in the identification of elements and resolving their relative content.

LPR conducted continuous measurements along the rover's 113-m traverse path during ~6.8 hours (Su et al. 2014). A total of 18,513 and 32,381 tracks of radar echo signals have been obtained for the first and second channel of LPR, respectively, providing ground penetrating radar data for the first time to analyze the depth of lunar regolith and subsurface structure.

EUVC has been imaging the terrestrial plasmasphere in 30.4 nm wavelengths during each lunar day, obtaining for the first time a lunar-based, wide-angle, continuous view of Earth's plasmasphere (Fig. 7). Until June 12, 2014, EUVC obtained more than 1,000 frames EUV images of Earth plasmasphere in 230 hours (Feng et al. 2014).

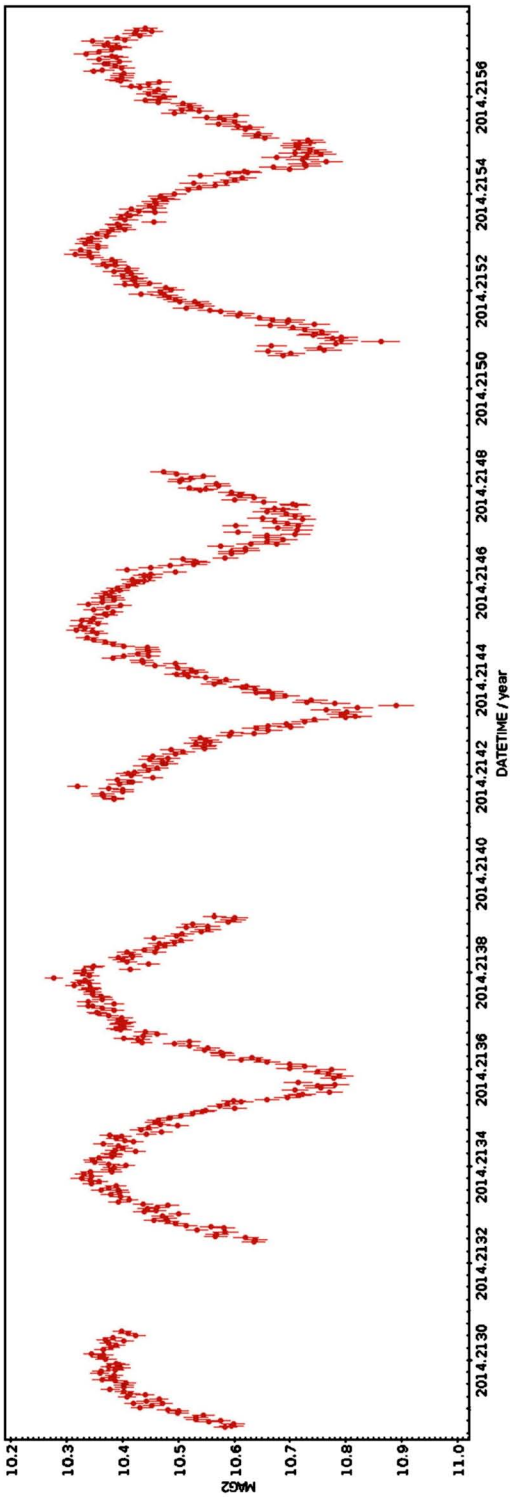

Fig. 8 Light curve of VW Cep double star

MUVT obtained night sky images in 245–340 nm wavelengths, employing both survey mode and target mode. The telescope has surveyed over 1,000 square degrees of the sky, while monitoring light curve changes of 10's of short-period variable stars by mid 2014 (Fig. 8). After calibration and background subtraction, NUV images of three sky areas near Draco were obtained and utilized to determine the celestial coordinates of target bodies.

7 Conclusion

The lander and EUVC and MUVT onboard are performing well. The rover traversed for a total of 114 m and stopped due to mechanical control issues toward the end of the second lunar day; science instruments onboard the rover are functioning well. With both the CE-3 lander and rover operating in long-term functioning mode, it is expected that CE-3 will be able to successfully accomplish its science objectives within its one-year nominal mission phase. The comprehensive data sets collected by the CE-3 science instruments will help improve our understanding of the compositional and geologic characteristics of and near the landing area, as well as the formation and evolution of Mare Imbrium and the Moon as a whole. The engineering capabilities demonstrated by CE-3 to successfully soft land on the Moon and deploy the rover promise great potential to eventually return lunar samples, which is the goal of Phase III of CLEP, in the future.

Acknowledgements We thank Julie Stopar for proofreading the manuscript that helped improve this paper and the two referees for their constructive comments.

References

B. Chen, K.F. Song, Z.H. Li, Q.W. Wu, Q.L. Ni, X.D. Wang, J.J. Xie, S.J. Liu, L.P. He, F. He, X.G. Wang, B. Chen, H.J. Zhang, X.D. Wang, H.F. Wang, X. Zheng, S.L. E, Y.C. Wang, T. Yu, L. Sun, J.L. Wang, Z. Wang, L. Yang, Q.L. Hu, K. Qiao, Z.S. Wang, X.W. Yang, H.M. Bao, W.G. Liu, Z. Li, Y. Chen, Y. Gao, H. Sun, W.C. Chen, Development and calibration of the Moon-based EUV camera for Chang'e 3. Res. Astron. Astrophys. **14**, 1654–1663 (2014)

G.Y. Fang, B. Zhou, Y.C. Ji, Q.Y. Zhang, S.X. Shen, Y.X. Li, H.F. Guan, C.J. Tang, Y.Z. Gao, W. Lu, S.B. Ye, H.D. Han, J. Zheng, S.Z. Wang, Lunar penetrating radar onboard the Chang'e-3 mission. Res. Astron. Astrophys. **14**, 1607–1622 (2014)

J.Q. Feng, J.-J. Liu, F. He, W. Yan, X. Ren, X. Tan, L.-P. He, B. Chen, W. Zuo, W.-B. Wen, Y. Su, Y.-L. Zou, C.-L. Li, Data processing and initial results from the CE-3 Extreme Ultraviolet Camera. Res. Astron. Astrophys. **14**, 1664–1673 (2014)

X.-H. Fu, C.-L. Li, G.-L. Zhang, Y.-L. Zou, J.-J. Liu, X. Ren, X. Tan, X.-X. Zhang, W. Zuo, W.-B. Wen, W.-X. Peng, X.-Z. Cui, C.-M. Zhang, H.-Y. Wang, Data processing for the active particle-induced X-ray spectrometer and initial scientific results from Chang'e-3. Res. Astron. Astrophys. **14**, 1595–1606 (2014)

W.D. Gonzalez, B.T. Tsurutani, A.L. Clua de Gonzalez, Interplanetary origin of magnetic storms. Space Sci. Rev. **88**, 529 (1999)

Z.P. He, B.Y. Wang, G. Lü, C.L. Li, L.Y. Yuan, R. Xu, B. Liu, K. Chen, J.Y. Wang, Operating principles and detection characteristics of the visible and near-infrared imaging spectrometer in the Chang'e-3. Res. Astron. Astrophys. **14**, 1567–1577 (2014)

V. Kaydash, Y. Shkuratov, G. Videen, Landing of the probes Luna 23 and Luna 24 remains an enigma. Planet. Space Sci. **89**, 172–182 (2013)

C.L. Li, L.L. Mu, X.D. Zou, J.J. Liu, X. Ren, X.G. Zeng, Y.M. Yang, Z.B. Zhang, Y.X. Liu, W. Zuo, H. Li, Analysis of the geomorphology surrounding the Chang'e-3 landing site. Res. Astron. Astrophys. **14**, 1514–1529 (2014)

B. Liu, C.L. Li, G.L. Zhang, R. Xu, J.J. Liu, X. Ren, X. Tan, X.X. Zhang, W. Zuo, W.B. Wen, Data processing and preliminary results of the Chang'e-3 VIS/NIR Imaging Spectrometer In-situ Analysis. Res. Astron. Astrophys. **14**, 1578–1594 (2014a)

J.J. Liu, W. Yan, C.L. Li, X. Tan, X. Ren, L.L. Mu, Reconstructing the landing trajectory of the CE-3 lunar probe by using images from the landing camera. Res. Astron. Astrophys. **14**, 1530–1542 (2014b)

M. Mendillo, Storms in the ionosphere: patterns and processes for total electron content. Rev. Geophys. **44**, RG4001 (2006)

D.L. Murphy, R.R. Vondrak, Effects of levitated dust on astronomical observations from the lunar surface, in *Proc. 24th Lunar Planet. Sci. Conf.* (1993), pp. 1033–1034

X. Ren, C.L. Li, J.J. Liu, F.F. Wang, J.F. Yang, E.H. Liu, B. Xue, R.J. Zhao, A method and results of color calibration for the Chang'e-3 terrain camera and panoramic camera. Res. Astron. Astrophys., 1557–1566 (2014)

Y. Su, G.Y. Fang, J.Q. Feng, S.G. Xing, Y.C. Ji, B. Zhou, Y.Z. Gao, H. Li, S. Dai, Y. Xiao, C.L. Li, Data processing and initial results of Chang'e-3 lunar penetrating radar. Res. Astron. Astrophys. **14**, 1623–1632 (2014)

X. Tan, J.J. Liu, C.L. Li, J.Q. Feng, X. Ren, F.F. Wang, W. Yan, W. Zuo, X.Q. Wang, Z.B. Zhang, Scientific data products and the data pre-processing subsystem of the Chang'e-3 mission. Res. Astron. Astrophys. **14**, 1682–1694 (2014)

F.F. Wang, J.J. Liu, C.L. Li, X. Ren, L.L. Mu, W. Yan, W.R. Wang, J.T. Xiao, X. Tan, X.X. Zhang, X.D. Zou, X.Y. Gao, A new lunar absolute control point: established by images from the landing camera on Chang'e-3. Res. Astron. Astrophys. **14**, 1543–1556 (2014)

J. Wang, J.S. Deng, J. Cui, L. Cao, Y.L. Qiu, J.Y. Wei, Lunar exosphere influence on lunar-based near-ultraviolet astronomical observations. Adv. Space Res. **48**, 1927–1934 (2011)

W.B. Wen, F. Wang, C.L. Li, J. Wang, L. Cao, J.J. Liu, X. Tan, Y. Xiao, Q. Fu, Y. Su, W. Zuo, Data processing and initial results from the CE-3 extreme ultraviolet camera. Res. Astron. Astrophys. **14**, 1674–1681 (2014)

W.R. Wu, Z.Y. Pei, T.J. Liu (eds.), *Chang'e 3 Mission Technical Handbook* (China Astronautic Publishing House, Beijing, 2014)

H.B. Zhang, L. Zheng, Y. Su, G.Y. Fang, B. Zhou, J.Q. Feng, S.G. Xing, S. Dai, J.D. Li, Y.C. Ji, Y.Z. Gao, Y. Xiao, C.L. Li, Performance evaluation of lunar penetrating radar onboard the rover of CE-3 probe based on results from ground experiments. Res. Astron. Astrophys. **14**, 1633–1641 (2014)